Proceedings of ACIC 07
Advanced Composites in Construction
2nd – 4th April 2007, University of Bath, Bath, UK

COMPOSITE MATERIALS FOR THE STRUCTURAL STRENGTHENING OF REINFORCED MASONRY SHELLS

Barros, J.A.O.[1], Bonaldo, E. [2], Oliveira, J.T.[3]

[1,2,3] *Dep. of Civil Eng , School of Eng., Univ. of Minho, Azurém, 4810 058 Guimarães, Portugal*

Abstract: Since the 1950s, the Uruguayan engineer Eladio Dieste designed curved lightweight masonry shells of impressive span width, complex shape and high attractiveness. This structural system is composed of a top mortar cover, a layer of clay bricks, mortar joints, and steel reinforcement. For the permanent loads, this structural system has been working satisfactory, in spite of rebar corrosion being detected in some shells. However, if submitted to an earthquake of considerable magnitude, damage can be significant, and its rupture can even occur.

In the present paper, an effective strengthening technique, using carbon fibre reinforced polymer (CFRP) materials, was developed to significantly increase the ultimate load of damaged reinforced masonry shell structures. This strengthening system is composed by strips of wet lay-up CFRP sheet and prefabricated CFRP laminates. The sheet strips are bonded, with epoxy resin, to the top cracked concrete surface of the shell to increase its flexural resistance for the negative bending moments, while laminates are fixed, with epoxy adhesive, to the bottom of the reinforced concrete joints to increase the shell flexural resistance for the positive bending moments. This strengthening system was applied to a damaged shell, having resulted a significant increase in the service load and an increase of about 76% in the ultimate load. A monitoring system was installed to evaluate the applied force, the deflection in critical sections and the strains in the composite materials and in the steel reinforcement. The experimental research is described and the main results are presented and discussed.

Keywords: *Reinforced Masonry Shell, Strengthening, CFRP, Pultruded Laminate, Wet Lay-up Sheet.*

1 Introduction

In Europe, historical structures are requiring rehabilitation works. In this context, the arches and vaults built in masonry represent a significant parcel of these constructions. Therefore, safeguarding masonry structures requires definition and application of appropriate methodologies and technologies for their strengthening and restoration [1]. The present paper deals with the strengthening of a reinforced masonry shell using carbon fibre reinforced polymers (CFRP) systems. The construction technology of this masonry shell was developed in the ambit of ISOBRICK European research project, and is composed by a top concrete cover, a layer of hollow clay bricks, concrete joints, and steel reinforcement [2], see Fig. 1. In Fig. 2 a Spanish model of this system is shown. This type of construction was designed in the past by the well know engineer Eladio Dieste [3]. This Uruguayan engineer designed and built a significant number of curved masonry shells since the 1950s.

Since some of the shells designed by Dieste are now presenting some damages, and are susceptible to extreme load conditions such are the case of seismic and wind, the use of CFRP materials to develop effective strengthening techniques for this type of structures is explored in the present work. For this purpose, a reinforced masonry arch was tested in two phases. In the first one, an unstrengthened arch was loaded up to introduce a certain level of damage (concrete cracking and debond between clay brick units and concrete joints). After have been strengthened with the proposed CFRP-based technique, the arch was, in a second phase, tested up to its failure. The adopted strengthening strategy was composed by two CFRP systems: CFRP laminates on intrados (inner surface) at the longitudinal concrete joints to increase the resistant positive bending moment, and CFRP wet-lay up sheet on the top concrete cover, on extrados (outer surface) to increase the resistant negative bending moment.

In spite of the linear-elastic brittle failure behaviour of FRP materials, its use for the flexural strengthening of concrete and masonry structures has received an increasing interest from several researchers interested in strengthening existing structures [4-6]. Since cement based materials and clay brick units have low tensile strength and little post cracking residual strength, but relatively large compressive strength, FRP materials can

[1] Associate Prof., Dep. of Civil Eng. barros@civil.uminho.pt
[2] PhD Student, bona@civil.uminho.pt
[3] Post-Doc Student, juliana@civil.uminho.pt

provide significant increments in terms of load carrying and deflection capacity of laminar structures made by these types of materials, such is the case of the reinforced masonry shells investigated in the present work. For the case of brick masonry vaults, the presence of FRP strips applied at the intrados changes the mechanism of plastic hinges formation, since these composites materials can increase significantly the cross section resistant bending moment due to their capacity to sustain tensile stresses. According to Valluzi [5], depending on FRP strengthening configuration, three mechanism of rupture can occur when strips of FRP are applied in masonry arches: (1) masonry crushing, (2) FRP detachment and (3) sliding along a mortar joint due to the shear stresses. Due to the easiness of its application, FRP materials can be more competitive than conventional materials for the strengthening of these types of structures [5]. Therefore, the present work explores the possibilities of these strengthening materials for reinforced masonry shells [7].

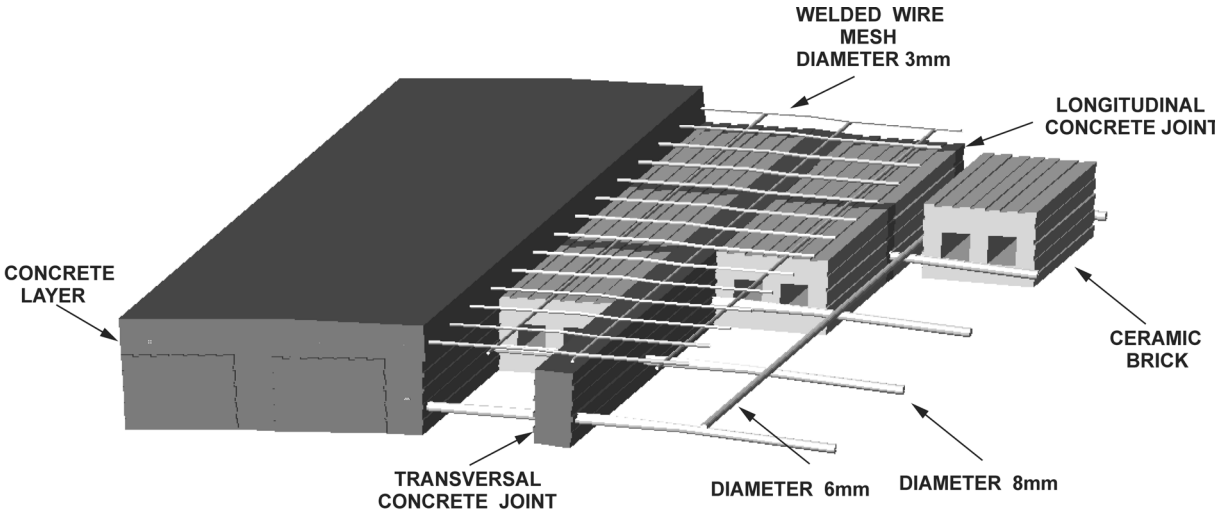

Figure. 1: Developed structural system

Figure. 2: View of the reinforced masonry shell system exposed in Spain

2 Structural System

The formwork of the built shell had a catenary geometrical configuration with a span of 4 m, a width of 1 m and a rise of 1 m (see Fig. 3). The hollow clay brick units average dimensions had 215 mm length, 100 mm width and 65 mm height (see Fig. 4), with square holes of 25 mm edge. Polystyrene pieces were introduced in the extremities of the brick holes to avoid excessive concrete penetration during the casting process of the shell. The concrete joints were reinforced with steel bars of ϕ8 mm and ϕ6 mm along directions orthogonal and parallel to the brick holes, respectively, see Fig. 1 and Figs. 3b and 3c. A welded wire mesh was placed in the top concrete cover and distanced of about 10 mm from the top surface of the brick layer. It was made of ϕ3 mm bars forming a square grid of 75 mm, see Fig. 1 and Figs. 3b and 3c. To reproduce the behavior of a masonry wall providing the restraining thrust to the arched shell two of ϕ10 mm steel bars were fixed in the extremities of the shell supports, see Fig. 3d. The formwork was removed twenty-four hours after the shell has been cast.

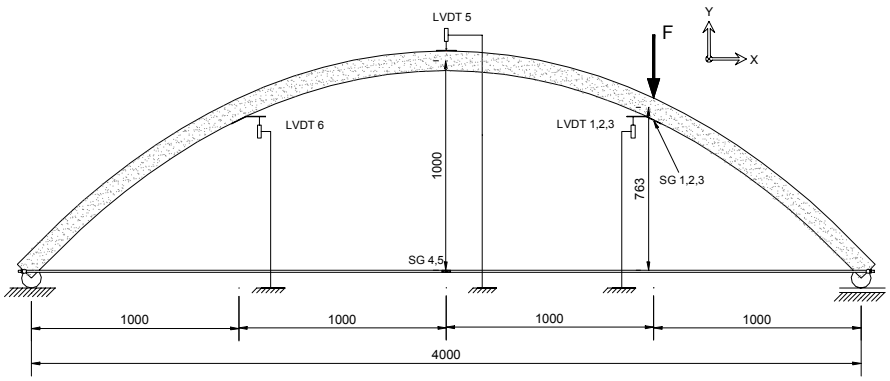

(a)

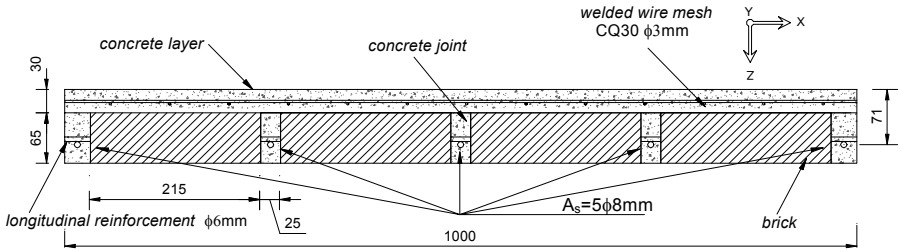

(b)

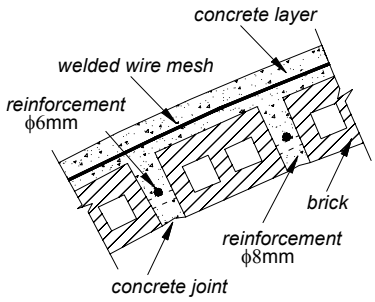

(c)

(d)

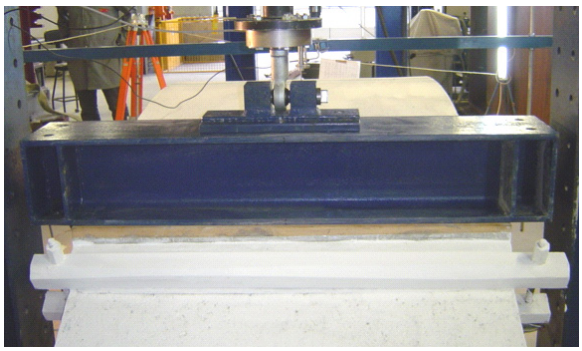

(e)

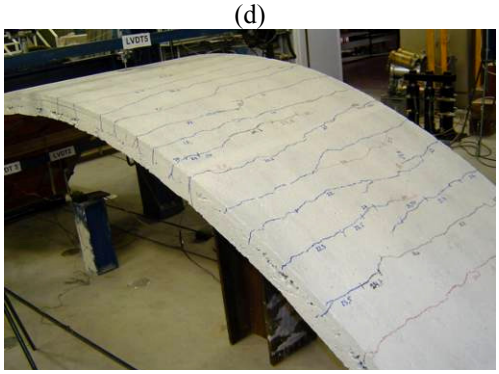

(f)

Figure 3: Masonry shell: (a) shell geometry; loading configuration and instrumentation; (b) shell cross section; (c) representative shell longitudinal section; (d) general view of the shell test setup; (e) loading devices; (f) crack pattern (dimensions in mm)

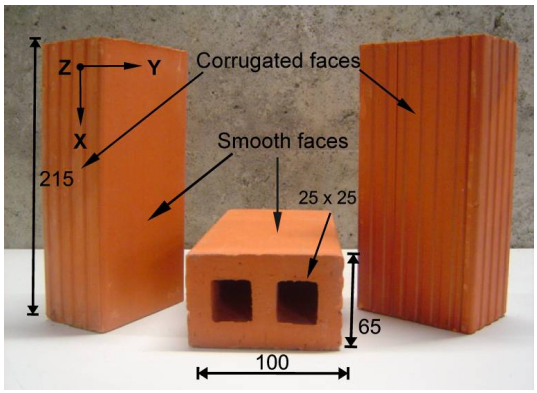

Figure 4: Brick dimensions in (mm)

3 Material Properties

3.1 Concrete

The mix composition of the concrete used in the built shell is included in Table 1. This mix was designed to provide a relatively low concrete strength class of appropriate workability and finishing requirements for the reinforced masonry shell. In fact the concrete would have enough fluidity to fill the joints and to assure good bond conditions with the reinforcements in the joints, and would have a viscosity level to avoid that concrete slides in the most inclined zones of the shell.

Compression cylinder tests in specimens of 150 mm diameter and 300 mm height and three-point bending tests with notched beams were carried out to characterize the concrete behavior in compression and in bending, respectively. The average results of concrete in compression and bending tests are included in Table 1 (f_{cm} = average compressive strength; $f_{fctm,fl}$ = average tensile strength in bending; G_f = average concrete fracture energy). The bending tests were carried out according to the RILEM TC 50 - FMC guidelines [8].

Table 1: Concrete properties

Material components		Composition (kg/m^3)	Average values of the mechanical properties		
			f_{cm} (N/mm^2)	$f_{fctm,fl}$ (N/mm^2)	G_f (N/mm)
Cement I 42.5 R		300	22.61 (*1.21*) [*5.36%*]	2.58 (*0.32*) [*12.57%*]	201.67 (*35.23*) [*17.47%*]
Fly-ash (FA)		30			
W/(C+FA)		0.54			
Fluvial sand	0.3 -0.6 mm	273			
	0.6-5 mm	710			
Gravel		872			
Superplasticizer GLENIUM ACE 32		1.5% of fine contents			

(*value*) - Standard deviation;
[*value*] - Coefficient of variation (COV) = (Standard deviation/Average) x 100

3.2 Clay Units

Due to the anisotropy associated with the extrusion processes of firing, the uniaxial compression tests were carried out in two orthogonal directions, namely along the length (X direction) and height (Y direction) [9,10], see Fig. 4. To limit the restraining effect of the machine steel loading platens, full units were used for testing in the X direction, while only half unit specimens were used for testing in the Y direction. The surfaces of the specimens in contact with the machine steel loading platens were ground to ensure planarity of these faces. The compressive strength of bricks loaded in X and Y directions, respectively, was 82 MPa and 32.8 MPa, respectively [9,10]. The compressive strength was obtained according to EN 772-1 [11]. The Young's modulus found for the bricks was 20 GPa [12]. A tensile strength of 1.3 MPa was obtained from direct tension tests in notched brick specimens [12]. These values represent, at least, the average of three specimens.

As mentioned before, polystyrene pieces were introduced in the ends of the brick holes to avoid excessive concrete penetration. In this way, part of the concrete of the transversal joints has penetrated (about 5 mm of penetration) into the brick holes, providing higher bond. The bond strength in this case was found equal to 0.9 MPa, while 0.25 MPa was the value found for the corrugated face [12].

3.3 Steel Bars and Wire Mesh

The steel bars were tested according to EN 10 002 - 1 recommendations [13]. The main results obtained from tensile tests in bar specimens of ϕ10 mm, ϕ8 mm, ϕ6 mm and ϕ3 mm are included in Table 2.

Table 2: Main properties obtained in tensile tests on steel bars couples

Bar diameter (mm)	Tensile stress at 0.2% (MPa)	Tensile strength (MPa)	Elasticity modulus (GPa)
3	545 (*29.50*) [*5.41%*]	824 (*56.31*) [*6.84%*]	200
6	672 (*57.16*) [*8.50%*]	676 (*65.57*) [*9.21%*]	217
8	489 (*33.78*) [6.90%]	579 (*23.14*) [*4.00%*]	195
10	377 (*21.59*) [*5.73%*]	484 (*7.50*) [*1.55%*]	213

(*value*) - Standard deviation
[*value*] - Coefficient of variation (COV) = (Standard deviation/Average) x 100

4 Testing and Main Results

4.1 Unstrengthened Masonry Shell

The shell was tested under monotonic vertical load applied at ¼ of its span (Fig. 3a and 3d) and distributed across the shell width, using a HEB 200 steel profile for this purpose (see Fig. 3e). The steel beam was supported on a wood beam (with a coin geometry) fixed with mortar to the top surface of the shell. The wood beam geometry was chosen to adapt the loading system to the shell curved geometry. The test was carried out under displacement control, using a servo-controlled test equipment, at a displacement ratio of 15 μm/s. One of the six displacement transducers was fixed to the servo-hydraulic actuator of 100 kN maximum capacity to control the test from the displacement of the piston of the actuator. The load was measured by a load cell of 200 kN capacity, attached to the actuator. Three displacement transducers, LVDT 1 – 3 were positioned along the shell width under the line load, see Fig. 3a. LVDT 5 was placed at mid span of the shell and LVDT 6 is at a symmetrical position of the line load. The shell was submitted to two monotonic loadings (c1 and c2). The c1 loading phase was interrupted when longitudinal reinforcement started yielding, see Fig. 5. The load in the shell was then removed. The second loading phase, c2, followed the same procedures of the first loading phase c1. Fig. 5 shows that, at about 15 kN a significant decrease of the shell stiffness occurred in the c1 loading phase due to the occurrence of damages such as, cracking of the concrete toping at the left part of the shell and cracking of the concrete joints under the line load, as well as, debonding between concrete joints and bricks at the region of the line load. The relationships between the applied force, *F*, and the average deflection at load line section, and between *F* and LVDT 6 show that in the c2 loading phase, up to a load of about 23 kN, the behaviour of the damaged shell was not so stiff than the one recorded in c1 loading phase, due to the fact that in the c2 loading phase the already cracked concrete and the already debonded concrete joints-bricks had a marginal contribution for the stiffness of the shell. However, after this load level, the deformational behaviour at both loading phases was almost similar, and the ultimate load of 29 kN was reached for both loading phases.

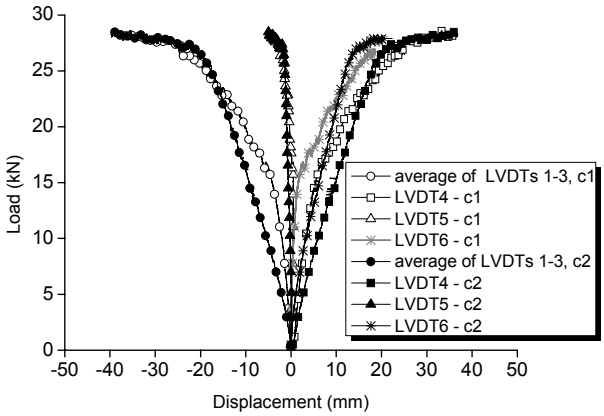

Figure 5: Relationship between displacements registered by LVDTs and the applied load (c1 - first loading and c2 - second loading)

Fig. 6 shows that, at the loaded section, the ϕ8 mm steel bars reinforcing the longitudinal concrete joints have yielded. The strain variation was only significant after a load level of about 10 kN, when the concrete of the joints started to cracking and the interface brick-concrete started to debond.

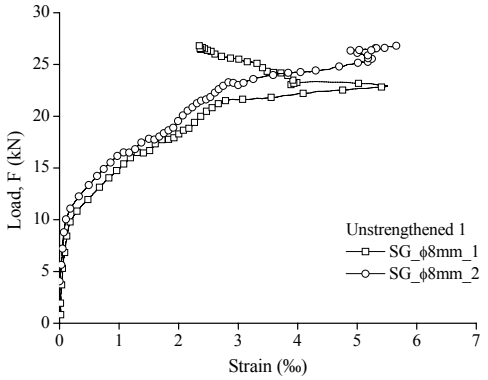

Figure 6: Relationship between the applied load and the strains in the internal steel ϕ8 mm bars

4.2 Strengthened Masonry Shell

The objective of the strengthening strategy was to provide for the damaged masonry shell an increase of 50% in its load carrying capacity that is the maximum increase level recommended by ACI 440 for the structural strengthening using composite materials

[14]. Two CFRP strengthening systems were used to accomplish this aim: wet lay-up unidirectional carbon fiber sheets with a Trademark "Mbrace® CF 130", and precured CFRP laminates with a Trademark "Mbrace Laminate LM". According to the supplier, these CFRP systems have the main properties included in Table 3. In the wet lay-up system, epoxy-based resins with Tradermaks "MBrace Resin 220, MBrace Resin 50 and MBrace Resin 55" were used as putty, primer and saturating resins, respectively. In the prefab system, the epoxy resin, adhesive MBrace Resin 50 and MBrace Resin 220 were used as primer resin and bonding adhesive, respectively. From experimental measures, a thickness of 1.411±0.013 mm and a width of 9.372±0.038 mm were obtained for the prefab laminates.

Using a cross-section layered model [4] that can evaluate the moment-curvature relationship of a cross-section, taking into account the constitutive laws of the intervening materials, the amount of CFRP laminates at the intrados (the positive moment region) and the amount of CFRP sheet at the extrados (the negative moment region) was computed to provide an increase in terms of these resisting moments that can assure an increment of, at least, 50% in the shell load carrying capacity. From this design two strips of CFRP sheet (t_f = 0.176 mm and w_f = 75 mm) were determined for the extrados and five CFRP laminates were obtained for the intrados.

Table 3: Properties of the CFRP systems

CFRP system			Main properties			
Type	Material		Tensile strength (MPa)	Young's modulus (GPa)	Ultimate strain (‰)	Thickness (mm)
Wet lay-up CFRP sheet	Primer		12	0.7	30	-
		[a]	5.9	0.33	52	
	Epoxy adhesive		54	3	25	-
		[a]	48.6	3.67	19	
	MBrace® CF 130		3800	240	15.5	0.176
		[a]	2862.9	218.4	13.3	0.180
Pultruded CFRP laminate	Epoxy adhesive		-	7	-	-
		[a]	33.0	7.5	4.8	-
	MBrace LM		2200	150	14	1.40
		[a]	2880	156.1	18.6	1.41[b]

[a] Evaluated from experimental tests carried out in the present research program; [b] Width of 9.37 mm

The following procedures were accomplished to apply the wet lay-up reinforcing system: 1) using a stone wear machine, a thin layer of concrete was removed in the zones where the CFRP strips would be installed; 2) using compressed air jet, the residues and dust were removed from the concrete surface; 3) using a spatula, the surface was regularized with putty paste; 4) a layer of primer was applied to enhance bonding; 5) the CFRP strips were fixed to the prepared concrete surface with the epoxy-based resin. These installation works are illustrated in Fig. 7. To apply the precured CFRP laminate strips the following steps were carried out: 1) using a disc sander machine, the longitudinal joints surface were regularized; 2) using compressed air jet, the residues and dust were removed from the joint; 3) using a brush, the surface was impregnated with the low viscosity coating; 4) the epoxy paste was applied and the laminates were fixed during the epoxy adhesive hardening phase. The application procedures of the precured CFRP laminates are shown in Fig. 8. Fig. 9 shows the strengthened masonry shell ready to be tested.

The experimental full-scale masonry shell strengthened at its intrados with CFRP laminate strips and at extrados with CFRP wet lay-up strips of sheet was tested under monotonic vertical line load. The general test scheme, disposition of the CFRP strengthening systems, arrangement of the LVDTs and strain gauges (SGs) applied to measure the shell deflection and the strains in the CFRP wet lay-up sheets, laminates and external steel bars are outlined in Fig. 10.

Three displacement transducers, LVDT 2, LVDT 3 and LVDT 4 were positioned along the masonry arch to measure displacements during the test. LVDT 2 was mounted under the arch at the loading line position. LVDT 3 was placed to register displacements at the central part of the shell, and LVDT 4 registered the displacements at ¼ of the shell span, in the opposite side of the loaded section. The test was carried out using the same equipment and equal test-control conditions, already described in section 4.1. Strain gauges were used to obtain information about the deformational behavior of the CFRP wet lay-up sheet, CFRP laminates and external steel bars. Four strain gauges (SG 1, 2, 3 and 4) were installed in the two CFRP strips, as is shown in Fig. 10. The four strain gauges were installed in the strips at the zone where the formation of cracks were firstly observed in the c1 loading phase of the unstrengthened shell

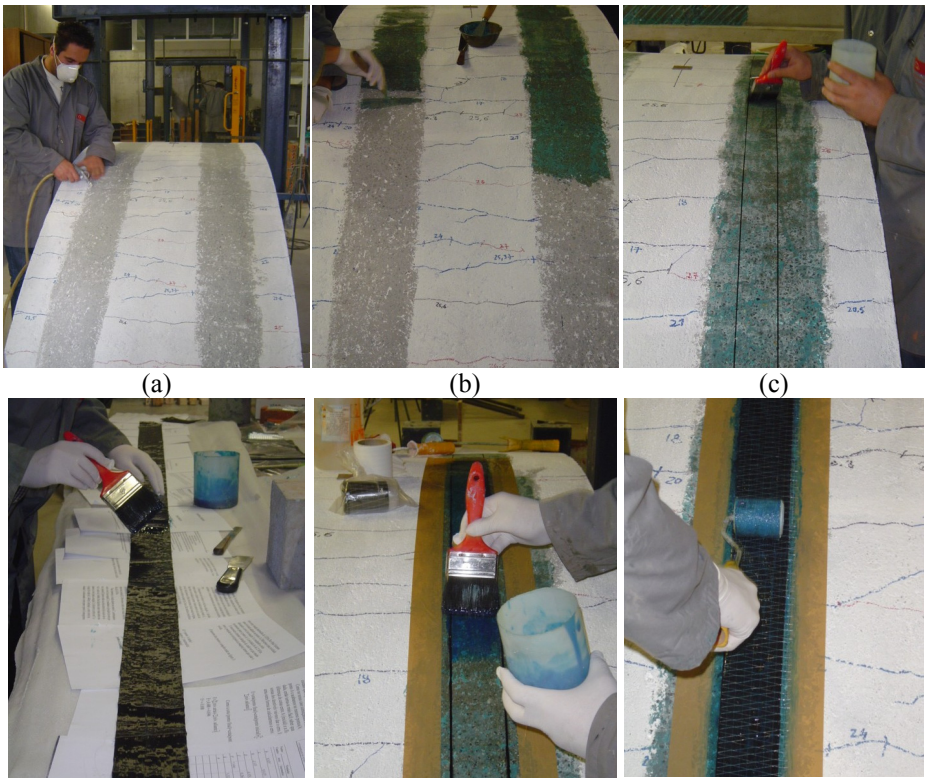

(a) (b) (c)

(d) (e) (f)

Figure 7: Wet lay-up main installation procedures: (a) cleaning the surface with compressed air jet, (b) applying repair putty, (c) area delimitation and primer application, (d) impregnating the CFRP strip with resin, (e) applying the resin on the primer cured surface, and (f) roller finishing

(a) (b) (c) (d)

Figure 8: CFRP laminates main installation procedures: (a) concrete joint surface preparation using a disc sander, (b) coating primer impregnating, (c) epoxy paste application, and (d) CFRP laminate positioning

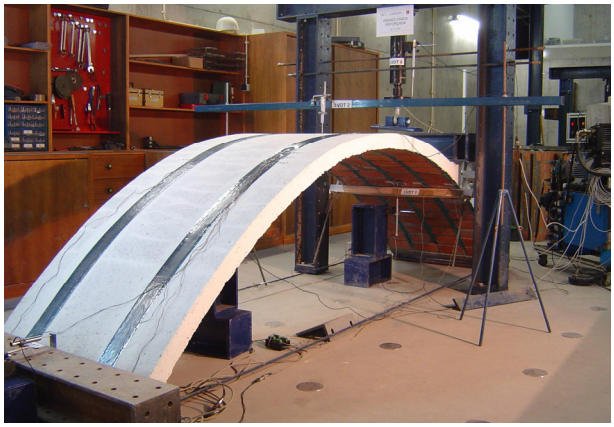

Figure 9: CFRP strengthened masonry shell

The two external steel bar ties (ϕ10 mm) of the masonry arch were also instrumented with one strain gauge per each tie (SG 8 and 9), at its central position (see Fig. 10).

During the test carried out with the unstrengthened shell, the SGs installed in two longitudinal steel bars (ϕ8 mm) were damaged. Therefore, the strain variation in these reinforcements was not available for the testing phase of the strengthened shell.

The strengthened shell presented the following failure mechanisms: detachment of the CFRP laminates (see Fig. 11a), crushing of the masonry clay units (see Fig. 11b), and the peel off of the wet lay-up strips of CFRP sheet (see Fig. 11c).

As already referred, the main purpose of this study is to assess the effectiveness of a CFRP strengthening technique to increase the load carrying capacity of reinforced masonry shell, when the strengthening procedures are applied in a shell that has intense damages. For the strengthened shell the maximum load was 51.05 kN, with displacements of 29.79 mm and 18.28 mm measured by LVDT 2 and LVDT 4, respectively (Fig. 12). The maximum load for the unstrengthened shell was 28.96 kN, at displacements of 35.07 mm and 18.84 mm, measured by LVDT 2 and LVDT 4 (that corresponds to the LVDT 6 in the unstrengthened shell, see Fig. 3a), respectively. Therefore, it was verified an increase of 76.28% in the shell maximum load, see Fig. 12.

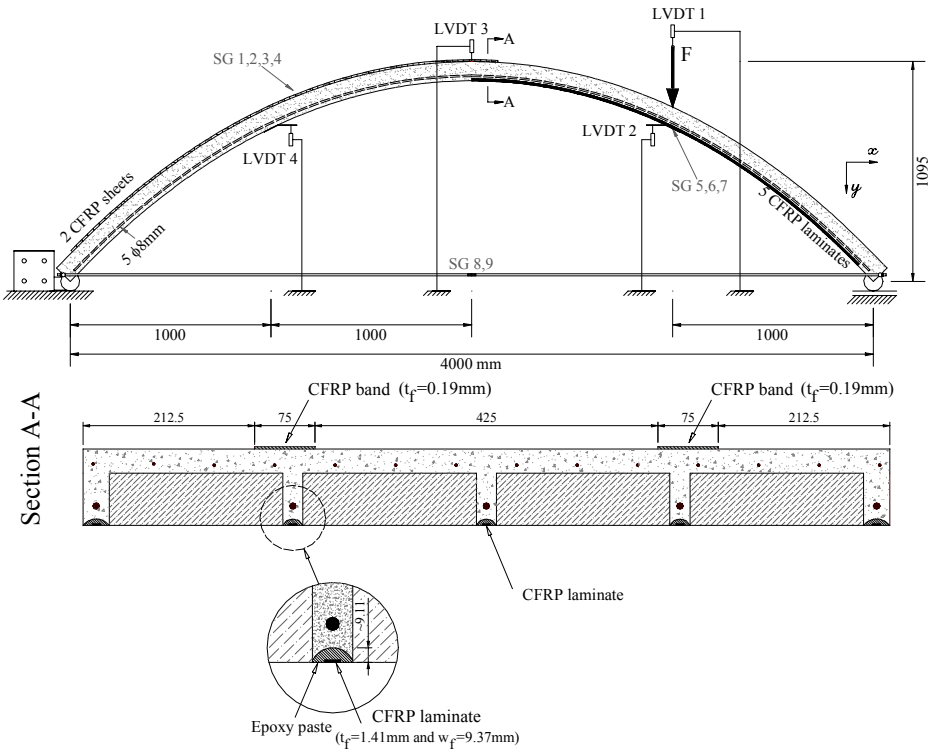

Figure 10: Test set-up and disposition of the CFRP strengthening

(a) (b) (c)

Figure 11: Failure mechanisms of the strengthened shell: (a) detachment of the CFRP strips; (b) crushing of brick units; (c) peeling of the CFRP strips

Fig. 13 represents the relationship between the applied load and the strains recorded in the SGs fixed on the CFRP materials. From Fig. 13a it can be observed that, when the wet lay-up strips of CFRP sheets were peeled off, the maximum strain was about 3.3‰ (22% of the ultimate strain of this CFRP material, Table 3). Fig. 13b shows that the strain variation during the loading procedure was almost uniform in the CFRP laminates, at the loading section. At the failure of the shell, the maximum strain was about 5.8‰ (31% of the ultimate strain evaluated in the tests carried out with this material, Table 3). In spite of the relatively reduced percentage of ultimate strain capacity installed in the CFRP materials in the test, the adopted strengthening strategy was able of exceeding the increment of shell load carrying capacity estimated when designing this CFRP strengthening configuration. It seems that a higher utilization of the CFRP materials could be achieved if a lower percentage of CFRP materials was used, since it might provide an ultimate load carrying capacity similar to the one obtained with

the adopted strengthening configuration, but with larger strain values in the CFRP materials.

Fig. 14 shows that the maximum strain installed in the steel ties was much lower than the yield strain of this material.

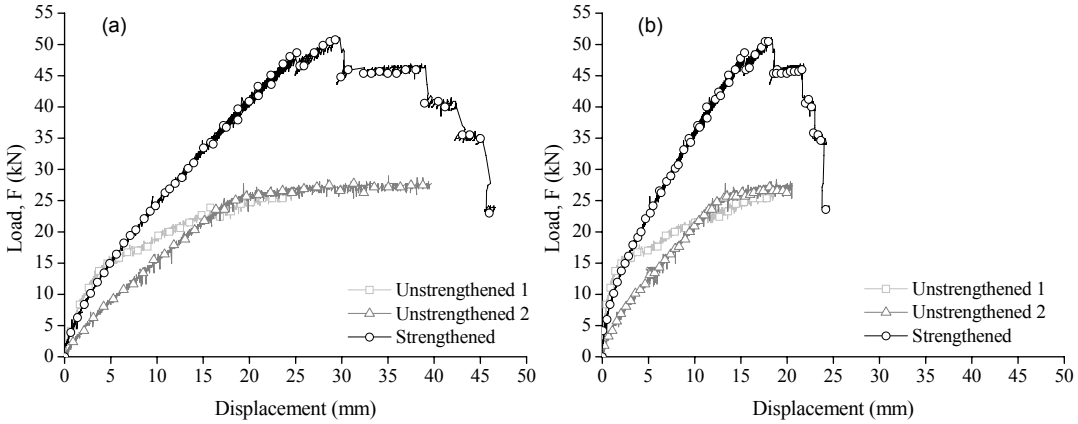

Fig. 12: Relationship between the applied load and the displacement measured by: (a) LVDT 2; (b) LVDT 4

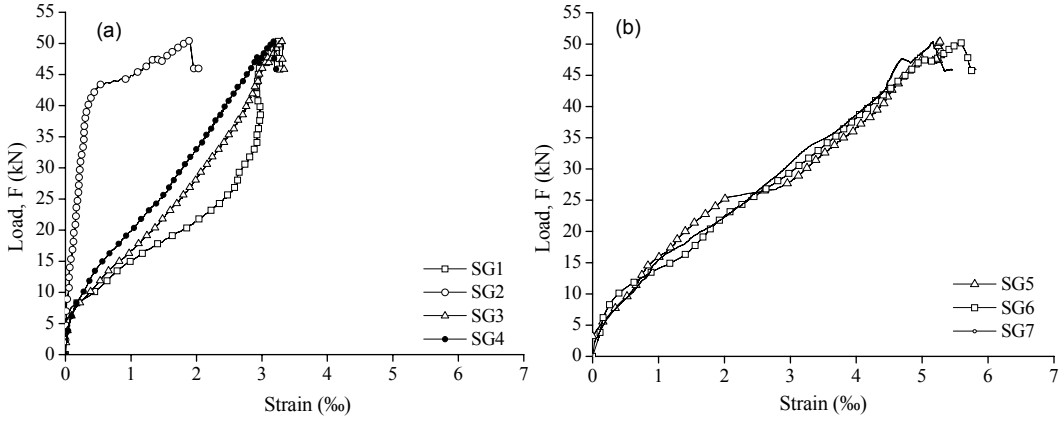

Figure 13: Experimental load-strain curves of: (a) CFRP strips of sheet and (b) CFRP laminates

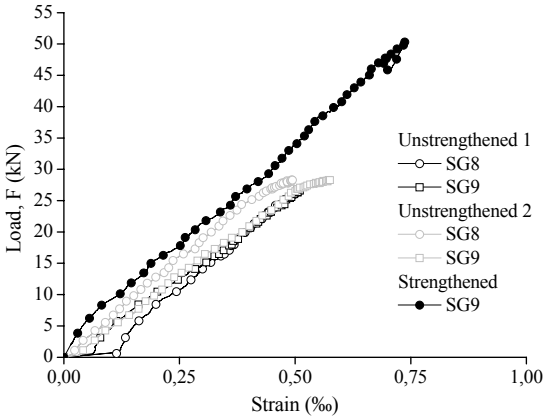

Figure 14: Experimental load-strain of steel ties

5 Conclusions

This paper presented a CFRP-based technique to strengthen damaged reinforced masonry shells. To assess the efficacy of the adopted strengthening technique, a reinforced masonry shell was built with a length of 4 m, a width of 1 m and a height of 1 m, and having a catenary geometry. The shell was composed by a layer of clay bricks involved by reinforced concrete joints, and covered by a reinforced concrete layer. The strengthening strategy consisted on fixing CFRP laminates in the shell intrados and strips of CFRP sheets in the shell extrados to increase the shell resistant positive and negative bending moments, respectively. The amount of CFRP materials was evaluated to increase the built shell load carrying capacity in 50%. For this purpose, it was used a cross section layer model, able of predicting the moment-curvature relationship of RC cross sections. In the first phase of the test program, the built shell was submitted to two cycles of monotonic vertical line load, applied to ¼ of the shell span. In each of these two cycles the load was applied up to the yield initiation of the longitudinal steel bars under the line load and extensive formation of cracks in the concrete cover layer. The main difference on the shell behaviour in these two loading cycles can be resumed to the loss of stiffness due to the cracking of the top concrete layer and longitudinal concrete joints, and due to debond between bricks and transversal concrete joints in the zone under the line load. However, the maximum load at these two cycles was similar, and equal to 29 kN for

a deflection of about 40 mm in the line load section. After have been strengthened with the adopted CFRP-based technique, the shell was tested under the same test conditions used the in first phase of the test program, and using similar monitoring system. From the obtained results it was verified that the stiffness of the undamaged shell was practically recovered and the ultimate load was 51 kN at a deflection of about 30 mm in the line load section. Three failure mechanisms occurred, in the following sequence: detachment of the laminates; crushing of some bricks; peeling-off of the strips of CFRP sheet. At the shell maximum load the maximum strains in the CFRP laminates and strips of CFRP sheet were 5.8‰ and 3.3‰, respectively. In spite of these relatively low values (31% and 22% of the corresponding ultimate strains), the adopted strengthened technique was able to provide an increase of 76% in terms of the shell load carrying capacity. However, it also seems to indicate that the amount of CFRP could have been lower without prejudicing the strengthening strategy in terms of shell stiffness and load carrying capacity.

Acknowledgments

This study is partly sponsored by a research program "Industrialized Solutions for Construction of Masonry Shell Roofs", supported by the European Commission. Acknowledgements are also due to SECIL, Bezerras' Quarry, S&P® Reinforcement and Bettor MBT Portugal. The second and third authors acknowledge the PhD grants supported by the Portuguese Science and Technology Foundation (FCT).

References

[1] Bati, S.B., Rovero. L., 2001. Experimental validation of a proposed numerical model for FRP consolidation of masonry arches, *Proceedings of the Historical Constructions*, Guimarães, Portugal, 1057-1066.

[2] Barros, J.A.O., Lourenço, P.B., Oliveira, J.T., Bonaldo, E. 2003. Contribution for a Full Prefabrication Approach of Masonry Reinforced Shells, Technical Report 03-DEC/E-05, Dep. Civil Eng., School of Eng., University of Minho, 15 p.

[3] Consejería de Obras Públicas y Transportes, 2001. *Eladio Dieste 1943-1996*, Sevilla, Montevideo, Dirección General de Arquitectura Y Vivienda - Junta de Andalucia, 306 p.

[4] Barros, J.A.O., Fortes, A.S., 2005. Flexural strengthening of concrete beams with CFRP laminates bonded into slits, *Journal Cement and Concrete Composites*, Vol. 27, No 4, 471-480.

[5] Valluzzi, M.R., Valdemarca, M., Modena, C., 2001. Behavior of Brick Masonry Vaults Strengthened by FRP Laminates, *Journal of Composites for Construction*, Vol. 5, No3, pp. 163-169.

[6] Ianniruberto, U., Rinaldi, Z., 2004. Ultimate Behavior of Masonry Arches Reinforced with FRP at the intrados - comparison between analytical and numerical models, *Proceedings of Structural Analysis of Historical Constructions*, Padova, Italy, 583-588.

[7] Barros, J.A.O.; Ferreira, D.R.S.M.; Fortes, A.S., Dias, S.J.E., 2006. Assessing the effectiveness of embedding CFRP laminates in the near surface for structural strengthening, *Construction and Building Materials Journal*, Vol. 20, 478-491.

[8] RILEM TC 50-FMC, 1985. Determination of fracture energy of mortar and concrete by means of three-point bend tests on notched beams, *Materials and Structures*, Vol. 18, No 106, 285-290.

[9] Oliveira, J.T., Barros, J.A.O., Lourenço, P.B., Bonaldo, E. 2003. Flexural Behavior of Reinforced Masonry Panels, Technical Report 03-DEC/E-12, Dep. Civil Eng., School of Eng., University of Minho, 76 p.

[10] Barros, J.A.O.; Oliveira, J.T.; Lourenço, P.J.B.; Bonaldo, E. 2006. Flexural behavior of reinforced masonry panels, *ACI Structural Journal*, Vol. 13, No. 3, May-June, 418-426.

[11] EN 772–1, 2000. CEN: Methods of test for masonry units – Part 1: Determination of compressive strength, Brussels, 14 p.

[12] Oliveira, J. T., 2005. Estudo experimental sobre a pré-fabricação de cascas de alvenaria cerâmica armada (Experimental study on the pre-fabrication of reinforced masonry shells), PhD Thesis, University of Minho, 2005. 246 p. (in Portuguese)

[13] EN 10 002–1, 1990. CEN: Metallic materials – Tensile testing. Part 1: Method of test (at ambient temperature), Brussels, 35 p.

[14] American Concrete Institute, 2002, Guide for the Design and Construction of Externally Bonded FRP Systems for Strengthening Concrete Structures, *ACI 440.2R-02*, Farmington Hills, MI, 118 p.